Redox Biology 69 (2024) 102993

Contents lists available at ScienceDirect

Redox Biology

journal homepage: www.elsevier.com/locate/redox

M^{6}A demethylase ALKBH5 regulates FOXO1 mRNA stability and chemoresistance in triple-negative breast cancer

Xi Liu [a,b,1], Pan Li [c,1], Yuanfeng Huang [c,1], Hongsheng Li [a], Xin Liu [a], Yaxi Du [a], Xin Lin [c], Danyang Chen [c], Hao Liu [c,*], Yongchun Zhou [a,b,**]

[a] Molecular Diagnosis Center, Third Affiliated Hospital of Kunming Medical University (Yunnan Cancer Hospital, Yunnan Cancer Center), Kunming, Yunnan, 650118, China
[b] Cancer Center Office, Third Affiliated Hospital of Kunming Medical University (Yunnan Cancer Hospital, Yunnan Cancer Center), Kunming, Yunnan, 650118, China
[c] Affiliated Cancer Hospital & Institute of Guangzhou Medical University, Guangzhou, Guangdong, 510095, China

ARTICLE INFO

Keywords:
Triple-negative breast cancer
Chemoresistance
ALKBH5
FOXO1
Reactive oxygen species

ABSTRACT

Resistance to chemotherapy is the main reason for treatment failure and poor prognosis in patients with triple-negative breast cancer (TNBC). Although the association of RNA N6-methyladenosine (m^{6}A) modifications with therapy resistance is noticed, its role in the development of therapeutic resistance in TNBC is not well documented. This study aimed to investigate the potential mechanisms underlying reactive oxygen species (ROS) regulation in doxorubicin (DOX)-resistant TNBC. Here, we found that DOX-resistant TNBC cells displayed low ROS levels because of increased expression of superoxide dismutase (SOD2), thus maintaining cancer stem cells (CSCs) characteristics and DOX resistance. FOXO1 is a master regulator that reduces cellular ROS in DOX-resistant TNBC cells, and knockdown of FOXO1 significantly increased ROS levels by inhibiting SOD2 expression. Moreover, the m^{6}A demethylase ALKBH5 promoted m^{6}A demethylation of *FOXO1* mRNA and increased *FOXO1* mRNA stability in DOX-resistant TNBC cells. The analysis of clinical samples revealed that the increased expression levels of ALKBH5, FOXO1, and SOD2 were significantly positively correlated with chemoresistance and poor prognosis in patients with TNBC. To our knowledge, this is the first study to highlight that ALKBH5-mediated *FOXO1* mRNA demethylation contributes to CSCs characteristics and DOX resistance in TNBC cells. Furthermore, pharmacological targeting of FOXO1 profoundly restored the response of DOX-resistant TNBC cells, both *in vitro* and *in vivo*. In conclusion, we demonstrated a critical function of ALKBH5-mediated m^{6}A demethylation of *FOXO1* mRNA in restoring redox balance, which in turn promoting CSCs characteristics and DOX resistance in TNBC, and suggested that targeting the ALKBH5/FOXO1 axis has therapeutic potential for patients with TNBC refractory to chemotherapy.

1. Introduction

Breast cancer is the most commonly diagnosed cancer and the leading cause of cancer-related deaths in women worldwide [1,2]. Triple-negative breast cancer (TNBC) is defined as the lack of expression of estrogen and progesterone receptors and human epidermal growth factor receptor 2 (HER2), accounting for approximately 15–20 % of all breast cancers. Compared to other subtypes, TNBC represents the most challenging subtype of breast cancer owing to its highly invasive nature, distant metastasis and recurrence, and lack of targeted therapy options. Chemotherapy is still the standard therapeutic treatment for patients with TNBC [3,4]. According to the National Comprehensive Cancer Network guidelines, doxorubicin (DOX) is the first-line drug used in adjuvant chemotherapy and postoperative complementary chemotherapy for patients with TNBC. About 30–50 % of patients with metastatic breast cancer who have not treated with chemotherapy are DOX responsive [5]. However, intrinsic or acquired drug resistance to DOX limited the efficacy of breast cancer treatment [6]. Therefore, there is an

* Corresponding author. Affiliated Cancer Hospital & Institute of Guangzhou Medical University, 78 Hengzhigang Rd, Guangzhou, Guangdong, 510095, China.
** Corresponding author. Molecular Diagnosis Center, Third Affiliated Hospital of Kunming Medical University, No.519 Kunzhou Road, Kunming, Yunnan, 650118, China.
E-mail addresses: liuhao@gzhmu.edu.cn (H. Liu), chungui7625@163.com (Y. Zhou).
[1] These authors contributed equally to this work.

https://doi.org/10.1016/j.redox.2023.102993
Received 3 November 2023; Received in revised form 6 December 2023; Accepted 7 December 2023
Available online 12 December 2023

urgent need to identify novel and effective therapeutic approaches to overcome this resistance, with the aim of eliminating mortality in patients with TNBC.

Reactive oxygen species (ROS) are oxygen free radicals, which are a series of oxygen products from oxidation-reduction reactions, including superoxide anions, hydrogen peroxide, and hydroxyl radicals [7]. In normal cells, ROS levels are balanced by elimination through antioxidant enzymes, such as superoxide dismutase (SOD), catalase, and peroxidase, which prevent oxidative damage to normal cells by oxygen free radicals [8]. Cancer cells exhibit enhanced ROS levels and increased dependence on the antioxidant defense system, which plays an important role in cancer initiation and progression [9]. Cancer cells are more sensitive to increased ROS levels than normal cells, and excessive ROS levels induced by chemotherapy or radiation can cause oxidative damage and induce cancer cell apoptosis [10]. In particular, the expression levels and activities of antioxidant enzymes in drug-resistant cancer cells are typically higher than those in non-resistant cancer cells, suggesting that cellular adaptation to ROS stress is critical for maintaining drug resistance. Therefore, the modulation of cellular ROS levels can enhance drug-resistant cancer cell death and sensitize them to chemotherapeutic drugs [11,12].

RNA N6-methyladenosine (m^6A) modification is one of the most pervasive and abundant RNA modifications and plays a critical role in regulating mRNA stability, splicing, transport, localization, and translation. The biological function of m^6A modification is dynamically and reversibly mediated by RNA m^6A methyltransferases, including methyltransferase-like (METTL)3, METTL14 and Wilms tumor 1-associated protein (WTAP), and m^6A demethylases, which includes fat mass and obesity-associated protein (FTO) and a-ketoglutarate-dependent dioxygenase AlkB homolog 5 (ALKBH5) [13,14]. Recent studies have suggested that the dysregulation of RNA m^6A methyltransferases/demethylases plays an important role in cancer initiation, progression, and metastasis by modulating the mRNA metabolism of oncogenic and tumor-suppressive transcripts. Dynamic RNA m^6A modifications are associated with therapy resistance, including drug transport and metabolism, target receptors, cancer stemness, DNA damage repair, and cell death [15–18]. However, the role of m^6A modifications in the development of therapeutic resistance in breast cancer is not well documented.

The present study aimed to investigate the potential mechanisms underlying ROS regulation in DOX-resistant TNBC cells. We found that ALKBH5-mediated Forkhead box protein O1 (FOXO1) m^6A modification increased *FOXO1* mRNA stability and expression, resulting in an increased SOD2 expression and attenuated cellular ROS levels, which in turn promoting CSCs characteristics and DOX resistance in TNBC. Moreover, targeting FOXO1 significantly enhanced the DOX sensitivity of DOX-resistant TNBC cells both *in vitro* and *in vivo*.

2. Materials and methods

2.1. Cell culture and reagents

The human breast cancer cell lines BT549 and MDA-MB-231 were purchased from American Type Culture Collection (ATCC, VA, USA). The DOX-resistant MDA-MB-231/DOX, and BT549/DOX cells were successfully established by continually exposing MDA-MB-231 and BT549 cells, respectively, to a gradually increasing concentration of doxorubicin for more than 12 weeks. All the cells were cultured in RPMI 1640 medium (Invitrogen, Carlsbad, CA, USA) supplemented with 10 % fetal bovine serum (Gibco, Grand Island, NY, USA) and 1 % penicillin/streptomycin in a humidified atmosphere with 5 % CO_2 at 37 °C. The cells were authenticated by DNA profiling by short tandem repeat (STR) analysis.

2.2. RNA interference and plasmid transfection

Lentiviral vectors expressing nontargeting pLKO.1 control shRNA (SCH002), two shRNA constructs targeting ALKBH5-shRNA1 (TRCN0000064783) and -shRNA2 (TRCN0000064787) were obtained from Sigma-Aldrich (St. Louis, MO, USA). Short hairpin sequences against either the FOXO1 or the scrambled short hairpin RNA (shRNA) sequences were cloned into the GFP-labeled lentiviral vector GV102 (GENECHEM). The target sequences selected are: shControl, TTCTCCGAACGTGTCACGT; shFOXO1-1, CAGTCTGTCCGAGATCAGTAA; shFOXO1-2, AGCGGGCTGGAAGAATTCAAT. Expression plasmid for pCMV6-SOD2 (Cat. No RC202330), and pCMV6-XL5 empty plasmid was purchased from Origene (Rockville, MD). For cell transfection, Lipofectamine 2000 reagent (Invitrogen, Carlsbad, CA) was used according to the manufacturer's instructions. After 72 h transfection, stably expressing or knockdown cells were selected in RPMI 1640 medium containing 1 μg/mL puromycin.

2.3. Cell viability assay

Cells were plated into 96-well plates and then incubated with doxorubicin for 72 h. Cell viability was detected by MTS assay using CellTiter 96 Aqueous One Solution Cell Proliferation Assay (Promega, Madison, WI, USA), following the manufacturer's instructions.

2.4. Cell apoptosis assay

Cell apoptosis was determined by Annexin V-APC/PI apoptosis kit (Keygen Biotech, Nanjing, China), followed by flow cytometer analysis (BD FACSCanto II, BD biosciences) according to manufacturer's instructions. The percentages of apoptotic cells in the Annexin V^+/PI^- and Annexin V^+/PI^+ populations were determined.

2.5. Combination index analysis

For the combination index (CI) analysis, cells were planted into 96-well plates and then treated with a concentration gradient of AS1842856, DOX or their constant ratio combination for 48 h. The CI value of the combination of AS1842856 and DOX was calculated according to the Chou-Talalay method by CompuSyn software, with $CI > 1$, $CI = 1$, and $CI < 1$ indicating antagonism, an additive effect, and synergism, respectively.

2.6. $CD44^+CD24^{-/low}$ population analysis

CD44 and CD24 antibodies (BD Pharmingen, San Diego, CA, USA) were used to fractionate the $CD44^+CD24^{-/low}$ population. Cells were harvested by dissociation using 0.05 % trypsin/EDTA. 1×10^6 cells were resuspended in 200 μL HBSS with 2 % FBS and then stained with the proper amount of antibodies (according to the instruction sheet) for 30 min at 4 °C. Cells incubated with unconjugated antibodies were stained with secondary antibodies for another 30 min at 4 °C. $CD44^+CD24^{-/low}$ population were assayed with flow cytometry (BD FACSAria III, BD Bioscience, USA).

2.7. Mammosphere formation assay

Cells were plated in ultralow attachment 6-well plates and maintained in DMEM/F12 supplemented with B27, 20 ng/mL EGF, 20 ng/mL basic fibroblast growth factor (bFGF), and 4 mg/mL heparin for 14 days. The mammospheres were photographed using inverted microscope (Leica, Hamburg, Germany).

2.8. ROS production

Intracellular production of ROS was determined by using oxidation

sensitive fluorescent probe 5-(and-6)- chloromethyl- 2′,7′-dichlorodihydrofluorescein diacetate (CM-H2DCFDA). Cells were incubated with 5 μM oxidation sensitive probe CM-H2DCFDA for 30 min at 37 °C in serum-free RPMI 1640 medium. Then, cells were washed with PBS twice and suspended in 0.5 mL PBS. CM-DCF fluorescence was measured by flow cytometry.

2.9. Superoxide dismutase activity

The enzyme activities of superoxide dismutase (SOD) were determined using the commercial assay kits (Jiancheng Biochemical, Inc., Nanjing, China) following the manufacturer's protocol. The specific enzyme activities of SOD were expressed as U/mg protein.

2.10. Quantitative real-time PCR

Total RNAs of whole cell lysates were isolated using the RNA-easy Isolation Reagent (Vazyme, Nanjing, China). The purity and concentration of extracted RNAs were measured on a NanoDrop 2000 (Thermo Fisher Scientific, Waltham, USA). 500 ng of total RNAs was then reverse transcribed using the iScript™ cDNA synthesis kit (Bio-Rad Laboratories, Inc., Hercules, CA, USA) according to standard protocols. Quantitative real-time PCR was performed on cDNA samples using Brilliant III Ultra-Fast SYBR® Green QPCR Master Mix (Agilent Technologies), and the signal was detected with Light Cycler 480 II Real-Time PCR System (Roche, Switzerland). The PCR primers used were as follows: FOXO1 (forward, 5′-TTATGACCGAACAGGATGATCTTG-3′ and reverse, 5′-TGTTGGTGATGAGAGAAGGTTGAG-3′); SOD2 (forward, 5′-ATGTTGAGCCGGGCAGTGTG-3′ and reverse, 5′-GTGCAGCTGCATGATCTGCG-3′); Catalase (forward, 5′-GAACTGTCCCTACCGTGCTCGA-3′ and reverse, 5′-CCAGAATATTGGATGCTGTGCTCCAGG-3′); GAPDH (forward, 5′-TGGTATCGTGGAAGGACTCA-3′ and reverse, 5′-CCAGTAGAGGCAGGGATGAT-3′.

2.11. RNA stability assay

Cells were seeded in a 6-well plate and transfected with desired constructs as described above. After 24 h transfection, cells were treated with actinomycin D (2 μg/mL) for 0, 2, and 4 h before collection. Total RNAs were isolated for qRT-PCR analysis.

2.12. m^6A-RIP qPCR

Total RNA was extracted from cells under indicated treatment, and then treated with DNase (Sigma) to remove genomic DNA. After mRNA purification and fragmentation, the fragments were incubated with m^6A primary antibody for immunoprecipitation using a Magna MeRIP™ m^6A kit (Merck Millipore, MA, USA). Enriched m^6A modified mRNA was then detected by qRT-PCR.

2.13. Western blot assay

Cells were lysed by RIPA buffer (Beyotime Biotechnology, China). Total protein concentrations were detected by BCA Protein Assay Kit (Thermo Fisher, Waltham, MA, USA). Separated by 8–12 % SDS-PAGE, the proteins were then transferred to PVDF membranes. Blocked with 5 % skim milk, the membranes were incubated with primary antibodies overnight at 4 °C and then the secondary antibodies for 1h at room temperature. Bound antibodies were visualized by ECL reagents (Thermo Fisher). ALKBH5 (ab195377) antibody was purchased from Abcam (Cambridge, MA, USA). SOD2 (#13141), Catalase (#12980), P53 (#2527), NRF2 (#12721), FOXO1 (#2880), METTL3 (#96391), METTL14 (#51104), Cleaved Caspase-3 (#9664), Ki67 (#9449), and human β-actin (#4970) antibodies were purchased from Cell Signaling Technology (Beverly, MA, USA).

2.14. Tumor xenograft model in mice

6-week old immunodeficient mice (Guangdong Medical Laboratory Animal Center, Guangzhou, China) were selected for generating a subcutaneous xenograft model. MDA-MB-231/DOX cells were implanted subcutaneously into the immunodeficient mice. 7 days later, mice were randomly divided into 4 groups, administrated with vehicle control, FOXO1 inhibitor AS1842856 (20 mg/kg/day, i. p.), Doxorubicin (5 mg/kg/day, i. p.), and AS1842856 combined with Doxorubicin, respectively. Tumor formation was examined every 4 days. Tumor volume was calculated by the formula, $LW^2/2$. At the end of experiment, tumors were collected and weighed, and then were dissected for fixation and embedded in paraffin, and then were subject to immunohistochemistry. All the animal studies were performed in conformity to protocols authorized by the Animal Experimentation Ethics Committee of Guangzhou Medical University. Standard animal care and laboratory guidelines were followed according to the IACUC protocol.

2.15. Clinical samples

The clinical samples were collected prior to any therapeutic procedures at the Affiliated Cancer Hospital and Institute of Guangzhou Medical University. All samples were collected with informed consent from the patients and all examining procedures were performed with the approval of the internal review and ethics boards of the hospital. Tumor specimens from fifty TNBC breast cancer patients who had received Doxorubicin-based chemotherapy were acquired from the Affiliated Tumor Hospital of Guangzhou Medical University between 2011 and 2016. Thirty-one patients manifesting early relapse within 6 months after the last course of chemotherapy were defined as the chemotherapy-resistant group and nineteen patients with no recurrent disease during follow-up comprised the chemotherapy-sensitive group. The clinicopathological features of the two subgroups were matched, such as age, pathological stage, as shown in Table S1.

2.16. Immunohistochemistry (IHC) assay

The tissues after formalin-fixed and paraffin-embedded were cut into 4-μm sections. The specimens were deparaffinized in xylene and rehydrated using a series of graded alcohols after being dried at 62 °C for 2 h. The tissue slides were then treated with 3 % hydrogen peroxide in methanol for 15 min. To exhaust endogenous peroxidase activity, and the antigen were retrieved in 0.01 M sodium cirate buffer (pH 6.0) using a microwave oven. After preincubation in 10 % goat serum, the specimens were incubated with a primary Ab at 4 °C overnight. The tissue slides were treated with a non-biotin horseradish peroxidase detection system according to the manufacturer's instruction. Two independent individuals evaluated the results of IHC. The staining intensity was scored as 0 (no signal), 1 (weak), 2 (moderate), and 3 (marked). Percentage scores were designated as 1, 1–25 %; 2, 26–50 %; 3, 51–75 %; and 4, 76–100 %. The scores of each tumor sample were multiplied to generate a final score of 0–12, and the tumors were finally characterized as negative (−), score 0; lower expression (+), score $\leq$4; moderate expression (++), score 5–8; and high expression (+++), score $\geq$9. An optimal cutoff value was determined: a staining index of five or greater defines tumors of high expression, and four or lower for low expression.

2.17. Statistical analysis

All data were presented as the mean ± SD. Statistical analyses were performed using GraphPad Prism 6 and SPSS version 16.0. A chi-square test was used to analyze the relationship between genes expression levels. Student's t-tests were performed to calculate the p-value, and $p < 0.05$ was considered statistically significant.

3. Results

3.1. Chemotherapy-resistant TNBC displayed lower ROS levels

The DOX-resistant TNBC cell models (MDA-MB-231/DOX, BT549/DOX) was successfully established by continually exposing MDA-MB-231 and BT549 cells to gradually increasing DOX concentrations for 3 months. Compared with parental cells, MDA-MB-231/DOX and BT549/DOX cells are less sensitive to DOX treatment, exhibiting significantly higher cell viability (Fig. 1A) and less cell apoptosis (Fig. S1). Importantly, both MDA-MB-231/DOX and BT549/DOX cells exhibited notable cancer stem cell (CSC) features (Fig. 1B–C). CSCs are functionally defined by their capacity to drive tumor growth and therapy resistance [19]. Previously studies suggested that low levels of reactive oxygen species (ROS) are crucial for maintaining cancer stem cells (CSCs) characteristics and chemoresistance [12,20]. To evaluate ROS levels in DOX-resistant TNBC cells, we measured intracellular hydrogen peroxide levels using flow cytometry after staining with CM-H2DCFDA. MDA-MB-231/DOX and BT549/DOX cells exhibited lower levels of ROS than those in the parental MDA-MB-231 and BT549 cells, respectively (Fig. 1D–E). This was further confirmed using immunofluorescence analysis (Fig. 1F). Cancer cells have developed antioxidant mechanisms to protect themselves from oxidative stress by expressing various detoxifying enzymes such as SOD2 and catalase(8,9). We found that the expression of SOD2 was significantly upregulated in MDA-MB-231/DOX and BT549/DOX cells compared to those in the parental cells (Fig. 1G–H). Furthermore, we found that SOD2 enzyme activity was significantly increased in DOX-resistant TNBC cells (Fig. 1I). These findings suggest a link between lower ROS levels and DOX resistance in TNBC, indicating that TNBC may have a cell-intrinsic drug resistance mechanism related to redox homeostasis.

3.2. FOXO1 is required for redox homeostasis in chemotherapy-resistant TNBC

Several transcription factors, including Nrf2, p53, and FOXO1, regulate intracellular ROS levels, thereby protecting cancer cells from oxidative stress [21–24]. We then investigated the expression levels of Nrf2, p53, and FOXO1 in DOX-resistant TNBC cells. We found that the levels of FOXO1, but not those of Nrf2 or p53, were significantly increased in MDA-MB-231/DOX and BT549/DOX cells (Fig. 2A). To explore the role of FOXO1 in regulating ROS homeostasis related to DOX resistance in TNBC, we constructed stable FOXO1-depleted MDA-MB-231/DOX and BT549/DOX cells using two independent short hairpin RNA (shRNA) sequences (shFOXO1-1 and −2) (Fig. 2B–C). As expected, we found that the knockdown of FOXO1 decreased *SOD2* mRNA and protein expression (Fig. 2B–C), and significantly increased intracellular ROS levels (Fig. 2D). To further validate whether FOXO1 regulates ROS level in DOX-resistant TNBC cells via SOD2, we overexpressed SOD2 in FOXO1-knockdown MDA-MB-231/DOX and

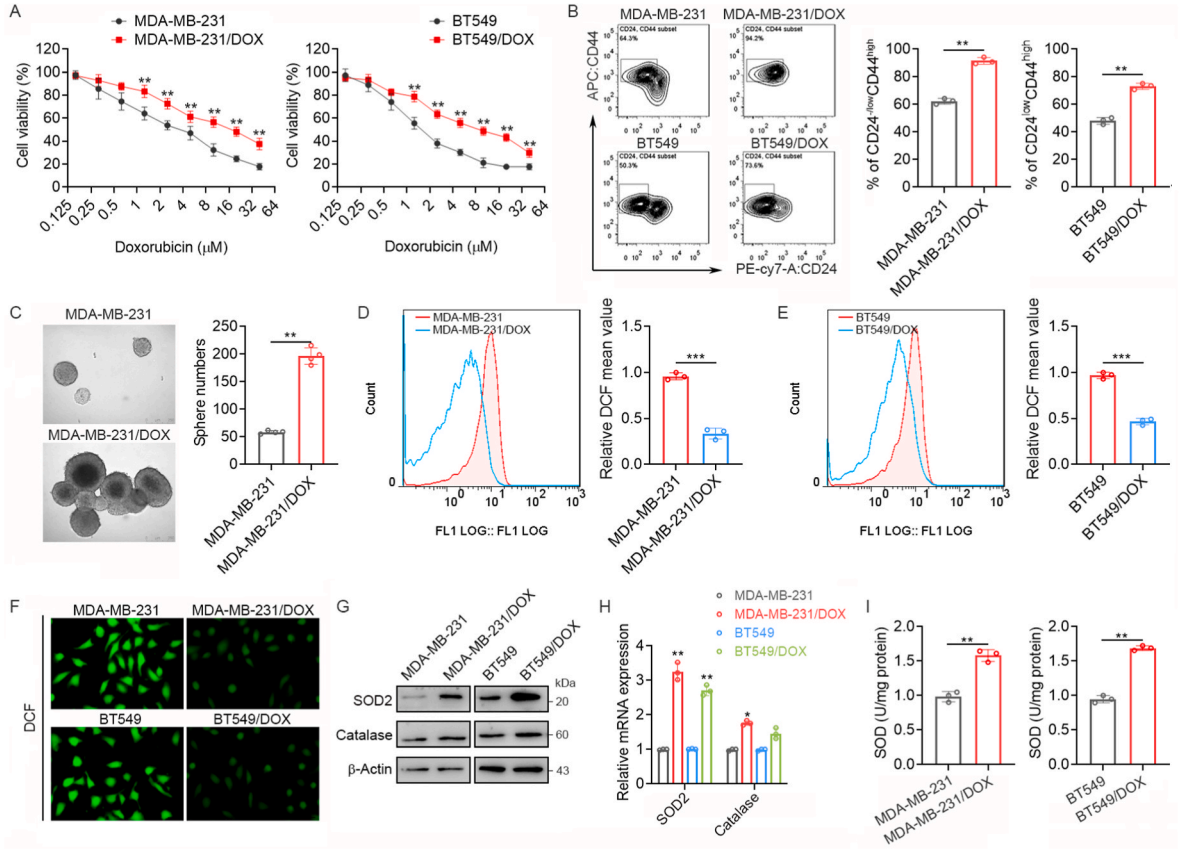

Fig. 1. Chemotherapy-Resistant Triple-Negative Breast Cancer (TNBC) displayed low reactive oxygen species (ROS) levels. (A) MDA-MB-231, MDA-MB-231/DOX, BT549, and BT549/DOX cells were treated with doxorubicin (DOX) at the indicated concentrations for 72 h, and cell viability was evaluated using MTS assays. (B) The percentages of $CD44^{+}/CD24^{-/LOW}$ cells in MDA-MB-231, MDA-MB-231/DOX, BT549, and BT549/DOX cells were measured by flow cytometry. (C) Self-renewal of CSCs in MDA-MB-231, and MDA-MB-231/DOX cells as measured by mammosphere formation assay. (D–E) ROS levels were analyzed using flow cytometry after exposing oxidation sensitive fluorescent probe (CM-H2DCFDA) in MDA-MB-231/DOX and MDA-MB-231 cells (D), BT549/DOX and BT549 cells (E). (F) Immunofluorescence was performed to analyze ROS levels in MDA-MB-231, MDA-MB-231/DOX, BT549, and BT549/DOX cells. (G–H) The expression levels of SOD2 and catalase in MDA-MB-231, BT549, MDA-MB-231/DOX, and BT549/DOX cells were determined using Western blot (G) and qRT-PCR (H), respectively. (I) The activities of SOD2 in MDA-MB-231/DOX and BT549/DOX cells were evaluated. Each point represents the mean ± standard deviation (SD). *$p < 0.05$, **$p < 0.01$, ***$p < 0.001$.

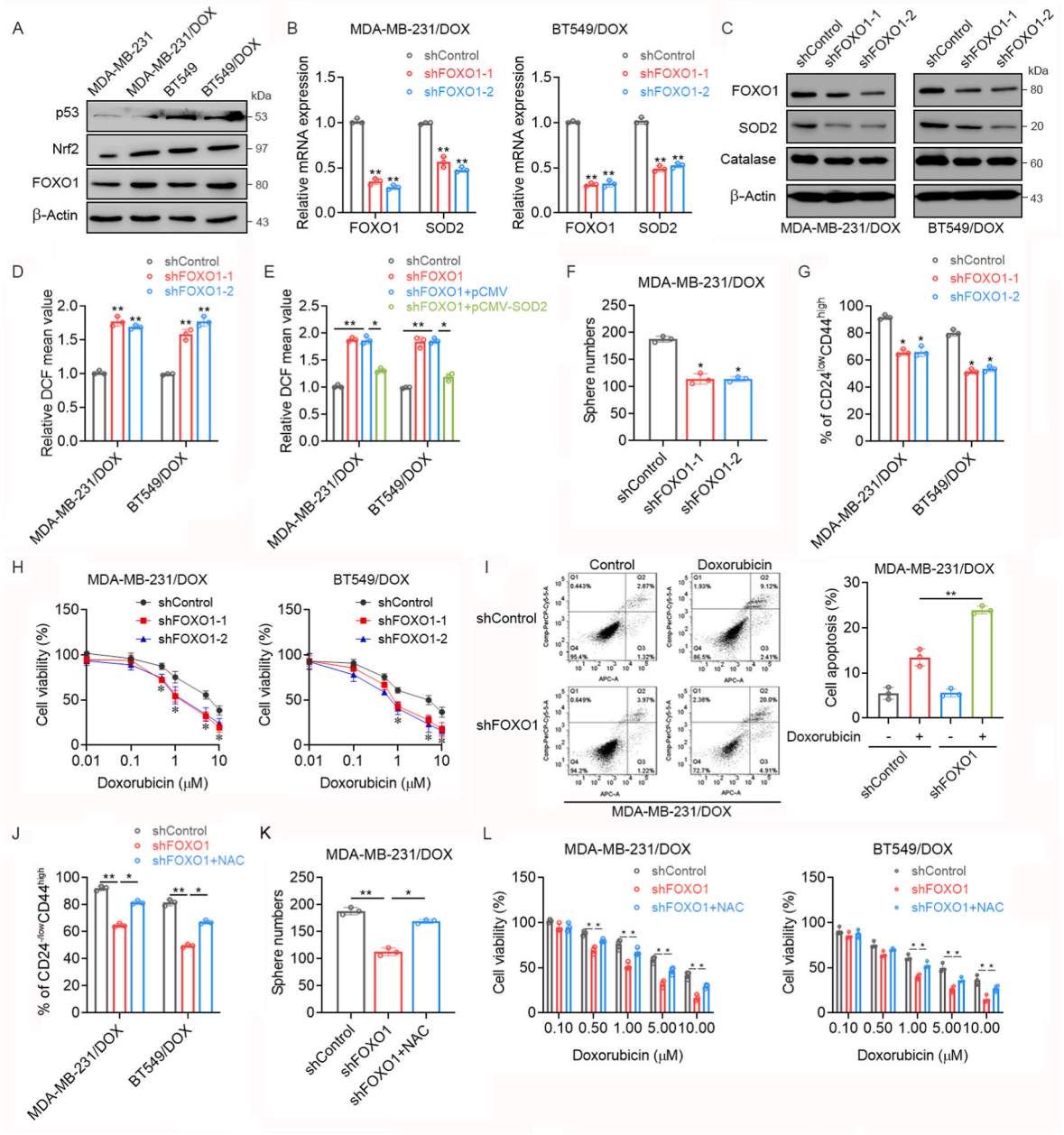

Fig. 2. FOXO1 is required for redox homeostasis in chemotherapy-resistant TNBC. (A) The expressions of p53, Nrf2, and FOXO1 in MDA-MB-231, BT549, MDA-MB-231/DOX, and BT549/DOX cells were determined using Western blot analysis. (B–C) MDA-MB-231/DOX and BT549/DOX cells were transfected with FOXO1 short hairpin RNA (shRNA) or control shRNA, the expressions of SOD2 and FOXO1 were determined using qRT-PCR (B) and Western blot (C). (D) MDA-MB-231/DOX and BT549/DOX cells were transfected with FOXO1 shRNA or control shRNA, the ROS levels were analyzed using flow cytometry. (E) MDA-MB-231/DOX and BT549/DOX cells were co-transfected with FOXO1 shRNA or control shRNA and pCMV or pCMV-SOD2, the ROS levels were analyzed using flow cytometry. (F) MDA-MB-231/DOX cells were transfected with FOXO1 shRNA or control shRNA, self-renewal of CSCs was measured by a mammosphere formation assay. (G) MDA-MB-231/DOX and BT549/DOX cells were transfected with FOXO1 shRNA or control shRNA, the percentages of $CD44^{+}/CD24^{-/low}$ cells were measured by flow cytometry. (H) MDA-MB-231/DOX and BT549/DOX cells transfected with FOXO1 shRNA or control shRNA were treated with DOX at the indicated concentrations for 72h; cell viability was evaluated using the MTS assay. (I) MDA-MB-231/DOX cells transfected with FOXO1 shRNA or control shRNA were treated with 2 μM DOX for 48 h; cells were then stained with Annexin V-APC and propidium iodide. Cell apoptosis was analyzed using flow cytometry. (J) MDA-MB-231/DOX and BT549/DOX cells transfected with FOXO1 shRNA were pretreated with 5 mM NAC for 24 h, the percentages of $CD44^{+}/CD24^{-/low}$ cells were measured by flow cytometry. (K) MDA-MB-231/DOX transfected with FOXO1 shRNA were pretreated with 5 mM NAC for 24 h, self-renewal of CSCs was measured by a mammosphere formation assay. (L) MDA-MB-231/DOX and BT549/DOX cells transfected with FOXO1 shRNA were pretreated with 5 mM NAC for 24h, and then treated with DOX at indicated concentrations for 72h, cell viability was evaluated by MTS assays. Each point represents the mean ± SD. *$p < 0.05$, **$p < 0.01$.

BT549/DOX cells (Fig. S2). As expected, SOD2 overexpression abrogated the FOXO1-knockdown-induced increase in ROS level (Fig. 2E). Notably, spheroid formation assays demonstrated that knockdown of FOXO1 decreased the spheroid-forming capacity of MDA-MB-231/DOX cells (Fig. 2F and Fig. S3A). Flow cytometry confirmed that breast cancer stem cell populations were reduced in the MDA-MB-231/DOX and BT549/DOX cells with *FOXO1* knockdown (Fig. 2G and Fig. S3B). Consistently, the knockdown of FOXO1 significantly increased sensitivity to DOX (Fig. 2H) and increased DOX-induced apoptosis in DOX-resistant TNBC cells (Fig. 2I). To assess whether the impact of

FOXO1 depletion on CSC properties and doxorubicin sensitivity is due to the increasing intracellular ROS, FOXO1-knockdown cells were treated with doxorubicin in the presence or absence ROS scavenger NAC. Our results showed that treatment of NAC reduced the ROS levels without affecting SOD2 expression (Fig. S4A–B). Importantly, we observed that NAC rescued breast cancer stemness in FOXO1-knockdown MDA-MB-231/DOX and BT549/DOX (Fig. 2J–K, Fig. S4C). Moreover, our results showed that NAC restored the DOX resistance of FOXO1-knockdown MDA-MB-231/DOX and BT549/DOX (Fig. 2L).

Previously studies suggested that FOXO1 is a transcriptional activator of drug efflux pump MDR1 [25], while increased MDR1 expression leads to chemoresistance in breast cancer cells [26]. Then, intracellular DOX concentration was measured to check whether the differential DOX response between FOXO1-knockdown MDA-MB-231/DOX and control cells was due to differential drug uptake or multidrug efflux pumps. When cells were treated with DOX at 5 μM, the intracellular DOX concentration of FOXO1-knockdown MDA-MB-231/DOX and control cells was detected and calculated based on the red fluorescence emitted from

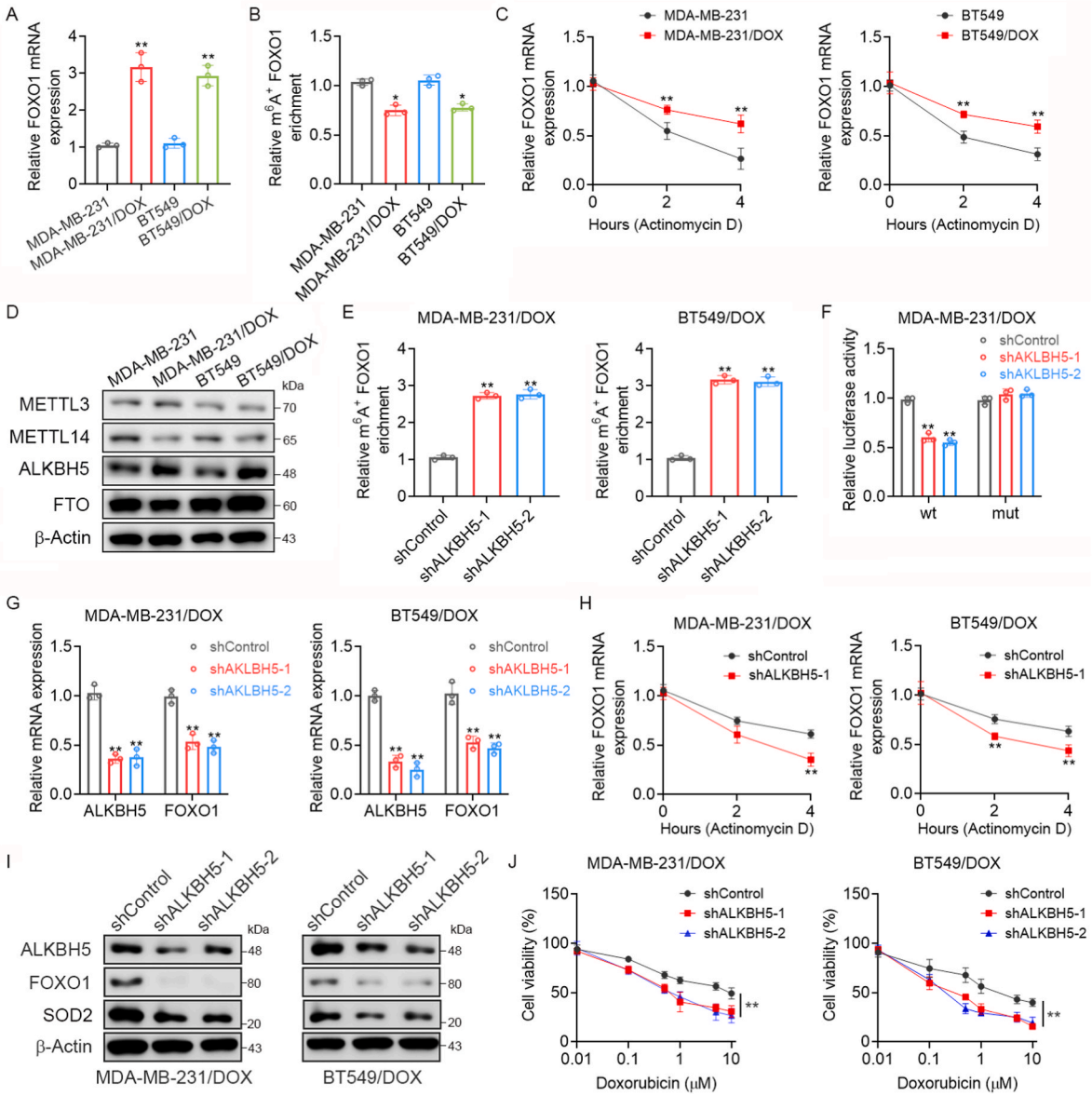

Fig. 3. ALKBH5 increased *FOXO1* mRNA stability in chemotherapy-resistant TNBC. (A) The expression levels of *FOXO1* mRNA in MDA-MB-231, BT549, MDA-MB-231/DOX, and BT549/DOX cells were determined using qRT-PCR. (B) M^6A immunoprecipitation (MeRIP)-qPCR assays were performed to determine the change of *FOXO1* mRNA with m^6A methylation in MDA-MB-231, MDA-MB-231/DOX, BT549, and BT549/DOX cells. (C) MDA-MB-231, BT549, MDA-MB-231/DOX, and BT549/DOX cells were treated with actinomycin D (2 μg/mL) at the indicated time points; the mRNA levels of *FOXO1* were determined using qRT-PCR. (D) The expression of m^6A modification-related protein METTL3, METTL14, ALKBH5, and FTO in MDA-MB-231, MDA-MB-231/DOX, BT549, and BT549/DOX cells were determined using Western blot. (E) MDA-MB-231/DOX and BT549/DOX cells were stably transfected with ALKBH5 shRNA or control shRNA, the m^6A modifications of *FOXO1* mRNA were measured by MeRIP-qPCR. (F) MDA-MB-231/DOX cells were co-transfected with ALKBH5 shRNA or control shRNA and wild-type (WT) or mutant (Mt) pmirGLO-FOXO1-3′-UTR reporter for 24 h, the relative luciferase activity was measured. (G) MDA-MB-231/DOX and BT549/DOX cells were transfected with ALKBH5 shRNA or control shRNA, the expression levels of ALKBH5 and FOXO1 were determined using qRT-PCR. (H) MDA-MB-231/DOX and BT549/DOX cells were transfected with ALKBH5 shRNA or control shRNA followed by treatment with actinomycin D (2 μg/mL) at the indicated time points; the mRNA levels of *FOXO1* were determined using qRT-PCR. (I) MDA-MB-231/DOX and BT549/DOX cells were transfected with ALKBH5 shRNA or control shRNA, the expression levels of ALKBH5, FOXO1, and SOD2 were determined using Western blot. (J) MDA-MB-231/DOX and BT549/DOX cells transfected with ALKBH5 shRNA or control shRNA were treated with DOX at the indicated concentrations for 72 h, cell viability was evaluated using the MTS assay. Each point represents the mean ± SD. *$p < 0.05$, **$p < 0.01$.

DOX. The result shows that the drug uptake curves were similar between FOXO1-knockdown MDA-MB-231/DOX and control cells without statistical differences, which excludes the decreased drug uptake as a major mechanism of FOXO1-induced DOX resistance in MDA-MB-231/DOX cells (Fig. S5). In summary, these data suggest that FOXO1 is a master regulator for reducing cellular ROS levels and restoring the redox balance in DOX-resistant TNBC cells, implying that FOXO1-mediated ROS downregulation is a mechanism underlying chemoresistance in TNBC.

3.3. ALKBH5-mediated m^{6}A demethylation increased FOXO1 mRNA stability in chemotherapy-resistant TNBC

We further investigated the potential mechanisms underlying FOXO1 upregulation in DOX-resistant TNBC cells. We found that *FOXO1* mRNA expression was significantly upregulated in MDA-MB-231/DOX and BT549/DOX cells (Fig. 3A). However, the luciferase reporter assay showed no significant change in FOXO1 promoter activity in DOX-resistant TNBC cells compared to that in the parental cells (Fig. S6A). Moreover, treatment with 5-aza-dC (a DNA methyltransferase inhibitor) or SAHA (a histone deacetylase inhibitor) had no significant effect on *FOXO1* mRNA expression in MDA-MB-231/DOX cells (Fig. S6B). RNA m^{6}A modification plays a critical role in regulating mRNA stability and expression. We evaluated the possible mechanisms involved in the m^{6}A-regulated expression of FOXO1 in DOX-resistant TNBC cells. Indeed, the reduction of m^{6}A-modified *FOXO1* mRNA in MDA-MB-231/DOX and BT549/DOX cells as compared to that in MDA-MB-231 and BT549 cells, respectively, was confirmed by the anti-m^{6}A immunoprecipitation (Fig. 3B). RNA stability assays revealed that *FOXO1* mRNA stability significantly increased in MDA-MB-231/DOX and BT549/DOX cells (Fig. 3C). Moreover, high ALKBH5 expression levels were observed in MDA-MB-231/DOX and BT549/DOX cells, whereas the protein levels of FTO, METTL3, and METTL14 were not consistently different between resistant and sensitive cells (Fig. 3D). Notably, we found that the m^{6}A-specific antibody significantly enriched *FOXO1* mRNA in ALKBH5-depletion MDA-MB-231/DOX and BT549/DOX cells (Fig. 3E). To study the role of ALKBH5-induced m^{6}A demethylation on the 3′-UTR of FOXO1, we generated luciferase reporters containing either wild-type (WT) FOXO1 3′-UTR or mutant 3′-UTR (GGACU to GGCCU) (Fig. S7A).

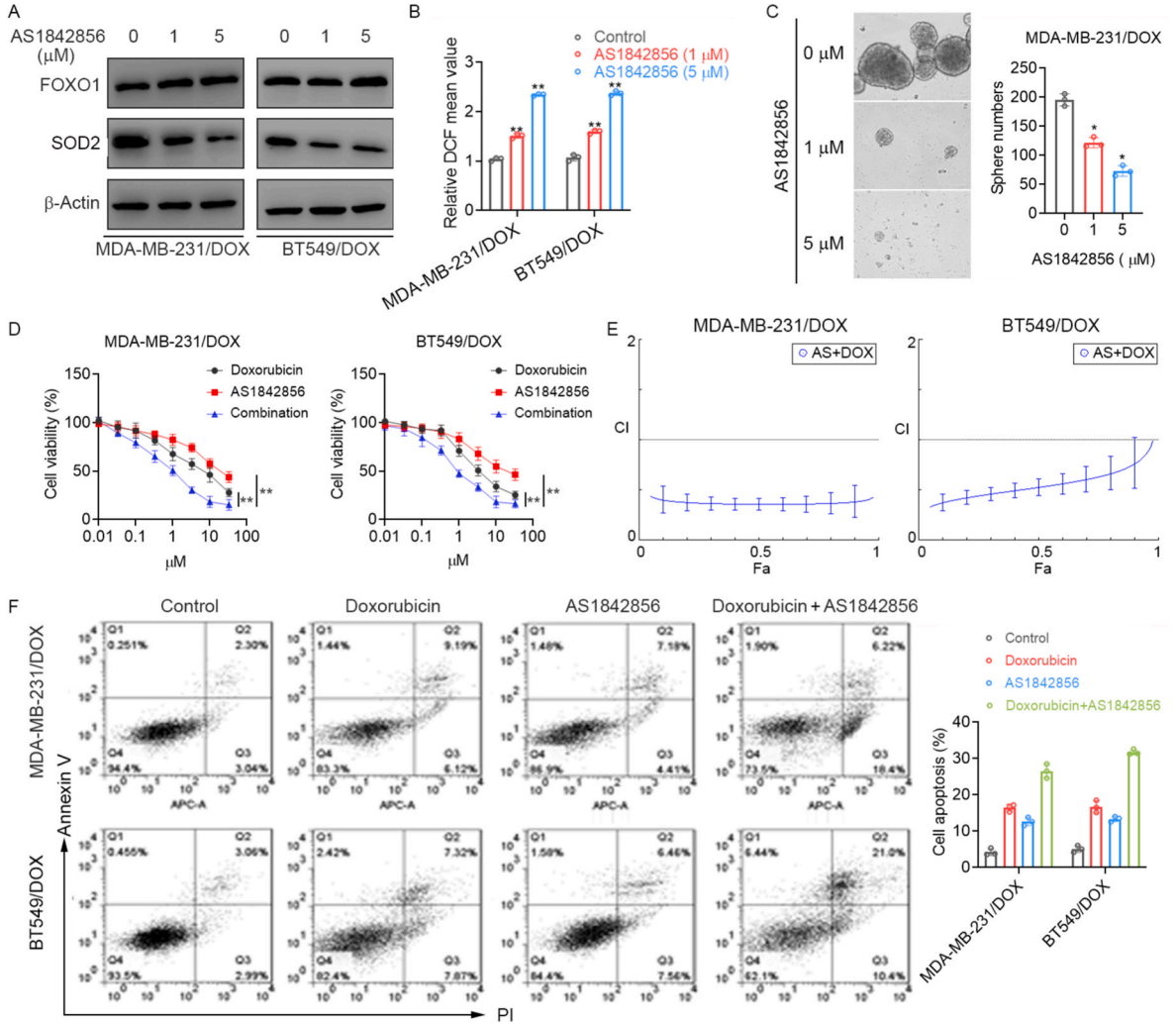

Fig. 4. Inhibition of FOXO1 abrogates chemoresistance in TNBC *in vitro*. (A) MDA-MB-231/DOX and BT549/DOX cells were treated with FOXO1 inhibitor AS1842856 at indicated concentrations for 48 h, the expression levels of FOXO1 and SOD2 were determined using Western blot. (B) MDA-MB-231/DOX and BT549/DOX cells were treated with FOXO1 inhibitor AS1842856 at indicated concentrations for 24 h, the ROS levels were analyzed using flow cytometry. (C) MDA-MB-231/DOX and BT549/DOX cells were treated with FOXO1 inhibitor AS1842856 at indicated concentrations, self-renewal of CSCs was measured by mammosphere formation assay. (D) MDA-MB-231/DOX and BT549/DOX cells were treated with DOX, AS1842856, or their combinations at the indicated concentrations for 72 h, cell viability was evaluated using MTS assays. (E) The combination index (CI) curves were calculated using the Calcusyn software, according to the Chou–Talalay equation. (F) MDA-MB-231/DOX and BT549/DOX cells were treated with 2 μM DOX in combination with 5 μM AS1842856 for 48 h, cells were then stained with Annexin V-APC and propidium iodide. Cell apoptosis was analyzed using flow cytometry. Each point represents the mean ± SD. *p < 0.05, **p < 0.01.

The luciferase assays showed that specific knockdown of ALKBH5 significantly inhibited WT-3′-UTR reporter activity, but had little effect on the luciferase activity of mutant-3′-UTR reporter (Fig. 3F, Fig. S7B), indicating that ALKBH5 was critically involved in *FOXO1* mRNA m^6A methylation. Furthermore, the specific knockdown of *ALKBH5* significantly reduced *FOXO1* mRNA expression and stability in MDA-MB-231/DOX and BT549/DOX cells (Fig. 3G–H), thus dramatically decreasing FOXO1 and SOD2 protein levels in MDA-MB-231/DOX and BT549/DOX cells (Fig. 3I). Importantly, the knockdown of ALKBH5 expression significantly increased DOX-mediated growth inhibition in both MDA-MB-231/DOX and BT549/DOX cells (Fig. 3J). Collectively, our data demonstrates the critical role of the ALKBH5-mediated *FOXO1* mRNA m^6A in developing resistance to chemotherapy in TNBC.

3.4. *FOXO1 inhibition abrogates chemoresistance in TNBC*

Considering that DOX-resistant TNBC cells have increased FOXO1 expression, it is conceivable to hypothesize that the therapeutic targeting of FOXO1 will overcome resistance and re-sensitize the cells to DOX-induced growth inhibition. To test this hypothesis, we used pharmacological approaches to suppress FOXO1 expression. AS1842856 has recently been identified as a potent inhibitor of FOXO1 that reduces DNA binding and transactivation ability [27]. Accordingly, the treatment of MDA-MB-231/DOX and BT549/DOX cells with AS1842856 potently decreased SOD2 expression (Fig. 4A), while increased intracellular ROS levels (Fig. 4B). Similar to FOXO1 depletion, treatment with AS1842856 also decreased the mammosphere formation potential in MDA-MB-231/DOX cells (Fig. 4C). Moreover, treatment of AS1842856 significantly enhanced DOX-induced growth inhibition in MDA-MB-231/DOX and BT549/DOX cells (Fig. 4D). To determine whether AS1842856 and DOX treatment have a synergistic inhibitory effect on cell growth, we performed the Fraction Affected-Combination Index plot (Fa-CI plot) analysis according to the Chou–Talalay equation [28]. The curves showed that the CI values were lower than 1.0 in combination of AS1842856 and DOX across a broad range of concentrations, suggesting that the combination of AS1842856 and DOX showed a synergistic inhibitory effect on the growth of MDA-MB-231/DOX and BT549/DOX cells (Fig. 4E). Flow cytometry was performed to confirm these results. DOX alone had a minor effect on inducing apoptosis in MDA-MB-231/DOX (total apoptotic cells

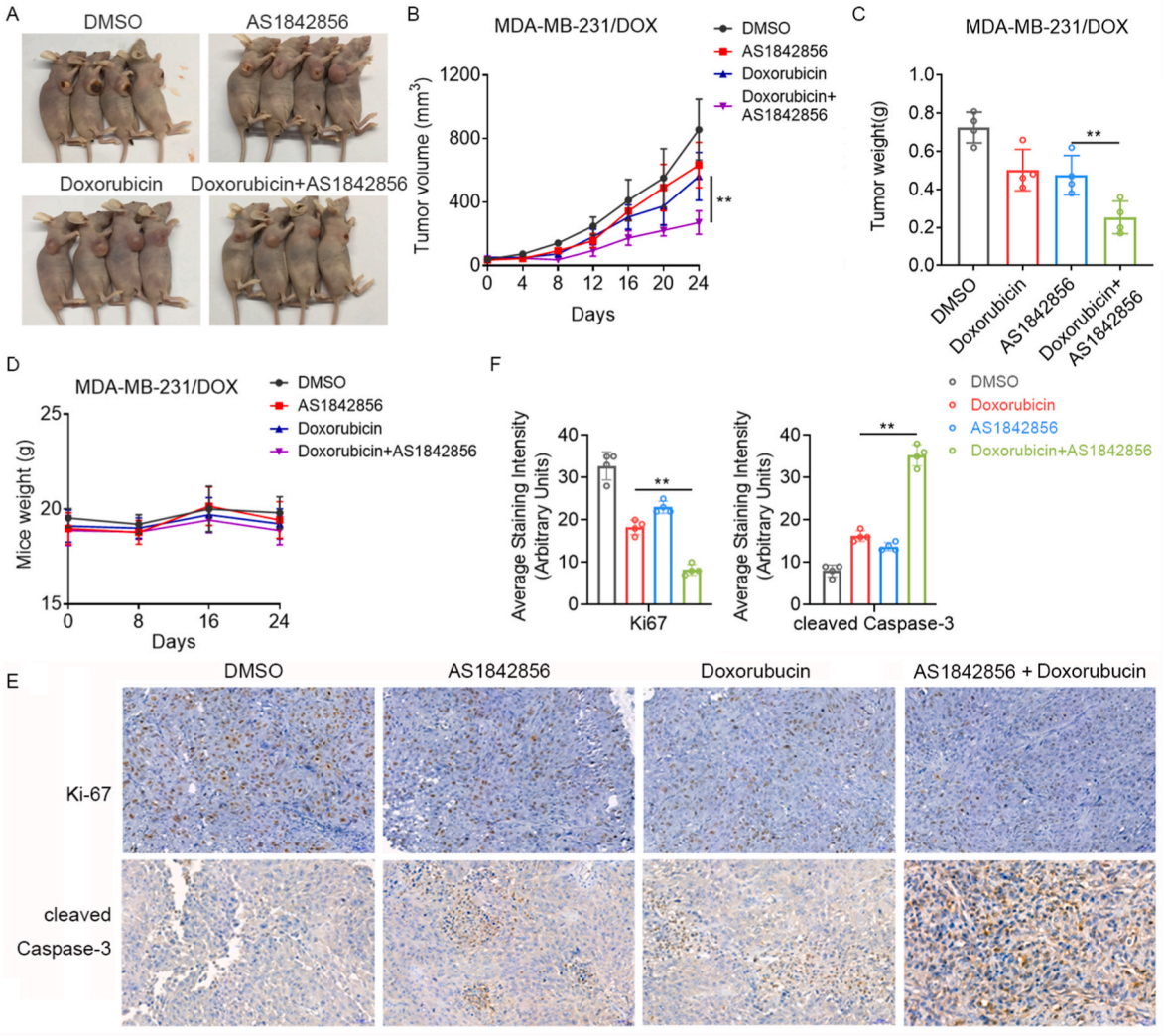

Fig. 5. Inhibition of FOXO1 abrogates chemoresistance in TNBC *in vivo*. (A–C) 5×10^6 MDA-MB-231/DOX cells were injected into nude mice and palpable tumors were allowed to develop for 7 days. Mice were randomly divided into four groups (n = 4) and treated with vehicle control (0.01 % dimethylsulfoxide in phosphate buffered saline), DOX (5 mg/kg/day, intraperitoneal (i.p.)), AS1842856 (20 mg/kg/day, i. p.) or a combination of DOX and AS1842856 every alternate day. (A–B) The tumor size was measured at indicated time intervals and calculated. (C) Measurement of tumor weights. (D) Body weight of the experimental mice during treatment. (E–F) Tumor tissues were fixed, sectioned, and placed on slides. Tumor specimens were subjected to immunohistochemical (IHC) staining for Ki-67 and cleaved caspase-3 (E), Quantification of IHC staining were analyzed by ImageJ and ImageJ plugin IHC profiler (F). Each point represents the mean ± SD. **p < 0.01.

approximately 15.2 %) and BT549/DOX (total apoptotic cells approximately 16.3 %) cells, whereas AS1842856 in combination with DOX dramatically increased the percentage of total cell apoptosis to 24.6 % and 31.4 % in MDA-MB-231/DOX and BT549/DOX cells, respectively (Fig. 4F).

To determine the anti-tumor activity *in vivo*, we tested the combinatorial effects of AS1842856 and DOX on tumor growth in a xenograft model. MDA-MB-231/DOX cells were inoculated into 6-week-old nude mice. After tumor formation, the tumor-bearing mice were treated with DMSO (control), AS1842856 (20 mg/kg/d), DOX (5 mg/kg/d), or a combination of AS1842856 and DOX. As expected, treatment with AS1842856 or DOX marginally reduced tumor growth; however, their combination inhibited tumor growth significantly (Fig. 5A–C). Moreover, all mice in each treatment group showed stable body weights, indicating that treatment with AS1842856, DOX, or their combination had no significant toxicity (Fig. 5D). Furthermore, immunohistochemical (IHC) assays revealed that the combination of AS1842856 and DOX considerably decreased cell proliferation and increased apoptosis in tumor xenografts (Fig. 5E–F). In summary, our data strongly support the hypothesis that FOXO1 inhibition overcomes DOX resistance and significantly enhances the efficacy of chemotherapy in TNBC.

3.5. *The clinical significance of ALKBH5/FOXO1/SOD2 axis in chemoresistance of TNBC*

To determine the clinical significance of the ALKBH5/FOXO1/SOD2 axis in the chemoresistance of TNBC, we collected and analyzed specimens from a cohort of 50 patients with TNBC who had received adjuvant treatments containing DOX. The expression of ALKBH5, FOXO1, and SOD2 in TNBC tissues was detected using IHC assays. We found that ALKBH5 was significantly upregulated in chemotherapy-resistant TNBC tissues (Fig. 6A–B). Consequently, the high expression of FOXO1 and SOD2 were significantly positively correlated with chemoresistance (Fig. 6A–B), and positively correlated with ALKBH5 expression (Fig. 6C). Moreover, we observed a significantly positive correlation between FOXO1 and SOD2 expression ($R = 0.42$, $p-value = 1.5e-47$), and ALKBH5 and FOXO1 expression ($R = 0.14$, $p-value = 6.6e-06$) in the TNBC tumors via Gene Expression Profiling Interactive Analysis (GEPIA) database (Fig. S8A). Moreover, Kaplan–Meier plotter analysis showed that the relapse-free survival (RFS) was shorter in TNBC patients with high ALKBH5 expression than in those with low ALKBH5 expression after administration with systemic chemotherapy. Similarly, patients with TNBC exhibiting increased FOXO1 and SOD2 expression showed reduced RFS ($P < 0.05$) (Fig. 6D). The prognostic values of ALKBH5, FOXO1, and SOD2 were further validated at the mRNA level in the cases from the Kaplan-Meier plotter dataset. We observed that higher levels of ALKBH5, FOXO1, and SOD2 were correlated with shorter survival in TNBC patients, but the correlation did not reach statistical significance (Fig. S8B). We next focused on whether ALKBH5, FOXO1, and SOD2 expression level in TNBC is correlated with the chemotherapy efficacy. We found that high expression of ALKBH5, FOXO1, and SOD2 was relevant to shorter survival in the chemotherapy group, but not in the non-chemotherapy group (Fig. S8C). In summary, these data suggest that the activation of ALKBH5/FOXO1/SOD2

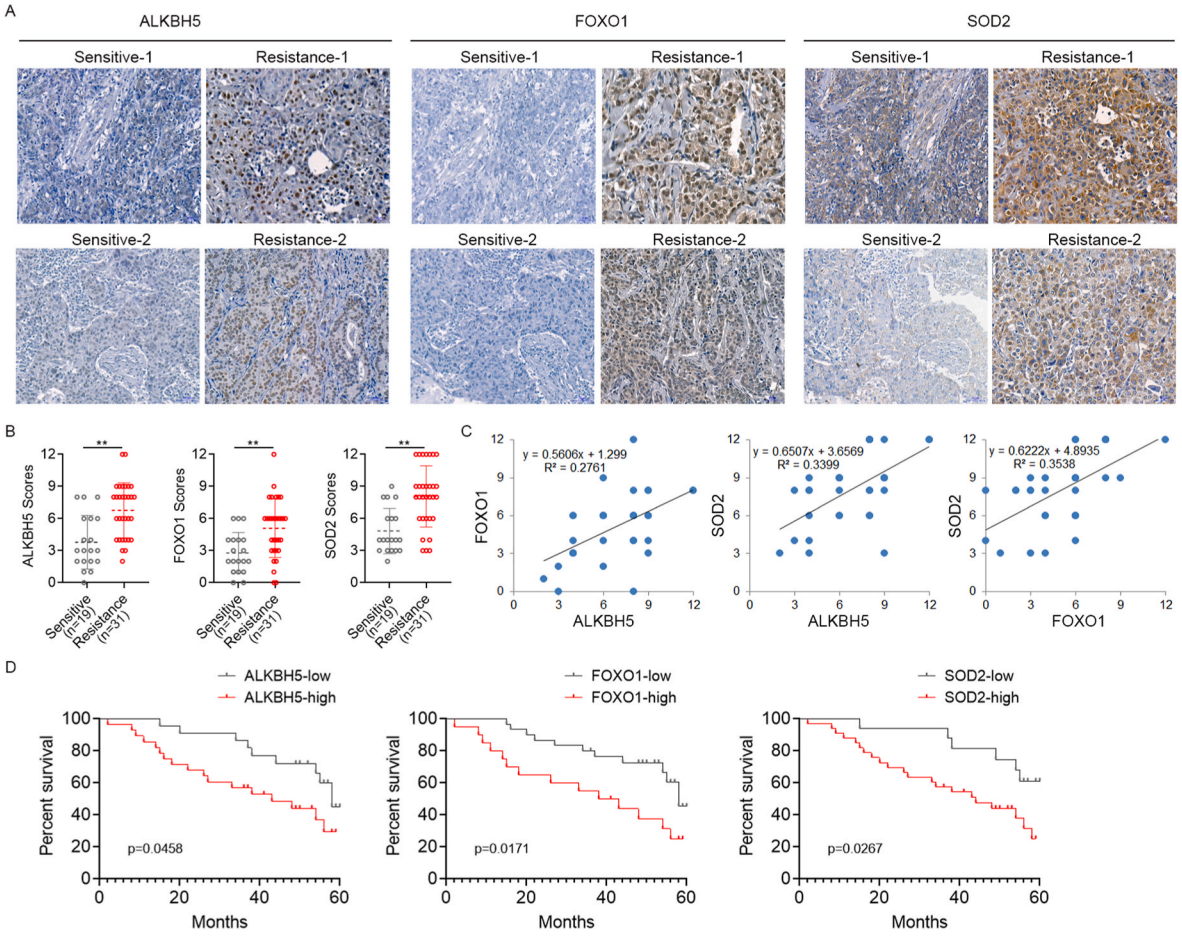

Fig. 6. The clinical significance of ALKBH5/FOXO1/SOD2 axis in chemoresistance of TNBC. (A) Representative images of ALKBH5, FOXO1, and SOD2 staining using IHC analysis in TNBC specimens. (B) IHC staining scores for ALKBH5, FOXO1, and SOD2 in chemotherapy-sensitive and chemotherapy-resistant TNBC specimens. (C) Correlation between the expression of ALKBH5, FOXO1, and SOD2 in TNBC tissues. (D) Kaplan–Meier analysis of relapse-free survival in patients with TNBC in relation to the expression of ALKBH5, FOXO1, and SOD2. Each point represents the mean ± SD. **$p < 0.01$.

signaling is a feature of acquired chemoresistance and could be used as a biomarker for chemoresistant TNBC.

4. Discussion

DOX is one of the common first line chemotherapeutic drugs used for TNBC treatment. However, intrinsic or acquired drug resistance to DOX limited the efficacy of TNBC treatment [29]. Studies on acquired DOX resistance have revealed that several mechanisms, including the ATP-binding cassette (ABC) membrane transporter family, altering in cell death, autophagy pathway, abnormal activation of signaling pathways, cell cycle arrest, epithelial to mesenchymal transition (EMT) and cancer stem cells (CSCs), have been reported in TNBC patients [30,31]. However, an optimal therapeutic strategy remains to be developed for TNBC patients with DOX resistance. M^{6}A is the most common and important RNA methylation modification and is recognized as a novel epigenetic regulator of RNA metabolism. M^{6}A modification is involved in various physiological and pathological processes, such as tumorigenesis, stem-like cell proliferation, and metastasis [15,32]. In this study, we identified a novel signaling pathway, involving m^{6}A demethylase ALKBH5, FOXO1 and SOD2, associated with DOX resistance. We demonstrated that the ALKBH5 plays a critical role in DOX resistance by regulating the FOXO1/SOD2 axis to maintain low ROS levels, which in turn promoting CSCs characteristics and DOX resistance in TNBC. Targeting FOXO1 effectively reversed DOX resistance both *in vitro* and *in vivo*. This study revealed a novel mechanism of DOX resistance in TNBC based on epigenetic insights.

Redox homeostasis is essential for maintaining the redox balance through ROS regulators in normal cells. Therefore, high levels of oxidative stress, a state of a disturbed balance between ROS production and the efficiency of antioxidants, have been detected in cancer cells [33,34]. Most conventional chemotherapeutic agents exert cytotoxic effects by inducing oxidative damage through ROS accumulation [35,36]. Chemoresistance results from the ability of cellular antioxidant programs to defend cancer cells against high ROS levels [37]. In this study, we found lower ROS levels in DOX-resistant TNBC cells than those in DOX-sensitive TNBC cells. Consistently, the remarkable antioxidant enzyme SOD2 was overexpressed in DOX-resistant TNBC cells. The specific mechanism for crosstalk between ROS level and chemoresistance remains poorly understood. Emerging evidence implied that ROS level regulates cancer stemness in a wide variety of cancers [38], whereas cancer stem cells have been considered to be associated with chemoresistance in TNBC [39]. Consistent with these observations, the results of our study demonstrated that lower ROS level played an essential role in stemness maintenance, which is responsible for DOX resistance in TNBC.

FOXO1, an intracellular transcription factor, is the main target of insulin signaling and regulates metabolic homeostasis in response to oxidative stress [40,41]. It plays a crucial role in regulating various cellular processes including cell cycle arrest, differentiation, apoptosis and DNA damage [42]. Several studies have also demonstrated that FOXO1 played an important role in protection of cancer cells against chemotherapy-induced apoptosis. For example, Pan et al. reported that AKT-mediated phosphorylation causes FOXO1 localization to the nucleus and increases pERK1/2 expression and drug resistance [43]. FOXO1 also contributed to chemoresistance in several cancer cells by activating FOXO1-related pathways, including AMPK, PI3K/AKT, JNK, and TGFβ1 signaling pathway [44,45]. In the present study, we demonstrated that FOXO1 silencing attenuated SOD2 expression while increased intracellular reactive oxygen species levels in DOX-resistant TNBC cells, which collectively suggested a direct role of FOXO1 in the development of chemoresistance through maintaining redox homeostasis in TNBC. Previous studies also suggested that FOXO1 may affect drug efflux pathway in breast cancer cells, which might be a major mechanism of doxorubicin resistance [25]. However, we found that the intracellular DOX uptake curves were similar between FOXO1-knockdown MDA-MB-231/DOX and parental cells, which excludes the decreased drug uptake as a major mechanism of FOXO1-induced DOX resistance in TNBC cells.

m^{6}A modification accounts for 80 % of RNA base methylation modifications and is the most abundant and reversible epigenetic modification in eukaryotes [13]. It is a dynamic balancing process regulated by RNA m^{6}A methyltransferases (METTL3, METTL14, and WTAP), demethylases (FTO and ALKBH5), and m^{6}A-binding proteins (YTHDC2, YTHDF1, and YTHDF2). Recently studies demonstrated the significances of ALKBH5 as an m^{6}A demethylase in the regulation of epigenetic processes and its effects on breast cancer progressions [46,47]. Our current data further our understanding of the function of ALKBH5 by proving its regulatory effect on the DOX resistance in TNBC. We observed that ALKBH5 was overexpressed in DOX-resistant TNBC cells. The upregulation of ALKBH5 was further confirmed in the clinical samples obtained from chemotherapy-resistant TNBC patients and was negatively correlated with RFS in the patients who received adjuvant treatments containing DOX. Moreover, we identified FOXO1 as one of the key downstream targets of ALKBH5. ALKBH5-mediated m^{6}A demethylation maintains FOXO1 overexpression in DOX-resistant TNBC cells through its impacts on mRNA stability. This is in agreement with the recent reports showing that m^{6}A modification acts as a crucial regulator of FOXO1 expression [48,49]. Similar to our findings, Yang et al. found that the m^{6}A demethylase FTO-induced mRNA expression of *FOXO1* was closely associated with glucose metabolism in patients with type 2 diabetes [50]. Moreover, our study clearly illustrated that specific knockdown of ALKBH5 significantly enhanced the sensitivity of DOX-resistant TNBC cells to DOX. To our knowledge, this is the first study to provide evidence that ALKBH5-mediated *FOXO1* mRNA demethylation contributes to redox homeostasis and chemoresistance in TNBC cells.

Finally, our findings suggested that ALKBH5/FOXO1/SOD2 axis may have predictive value for chemotherapy benefit, potentially minimizing the risk of development of chemotherapy resistance in TNBC. Although upregulation of ALKBH5, FOXO1, and SOD2 was relevant to shorter survival in the patients who received adjuvant chemotherapy, the upregulation of FOXO1 and SOD2 was found no notable correlation with OS in the non-chemotherapy group. Previously studies have demonstrated that upregulation of FOXO1 was responsible for not only the initial response to cancer therapeutics, but also the subsequent acquisition of therapeutic resistance [44,51,52]. Thus, the response of TNBC cells to chemotherapeutic agents, such as doxorubicin may depend on transient activation of ALKBH5/FOXO1, whereas sustained FOXO1 activation could paradoxically promote chemoresistance in TNBC via inducing SOD2 expression to maintain redox homeostasis and stemness. We postulated that ALKBH5 or FOXO1 inhibitors in combination with chemotherapeutic agents might be a valuable strategy for TNBC treatment. Indeed, our *in vitro* and *in vivo* data strongly support the hypothesis that FOXO1 inhibition overcomes DOX resistance and significantly enhances the efficacy of chemotherapy in TNBC.

5. Conclusion

Our findings reveal a novel mechanism of chemoresistance in TNBC cells mediated by m^{6}A modification through the ALKBH5/FOXO1/SOD2 axis (Fig. 7), providing a valuable strategy for overcoming chemoresistance by targeting FOXO1 through combination therapy in patients with TNBC.

Funding

This work was supported by Yunnan Fundamental Research Projects (202201AY070001-164), the National Natural Science Foundation of China (82172810, 82373088), the Guangdong Basic and Applied Basic Research Foundation (2023A1515010097).

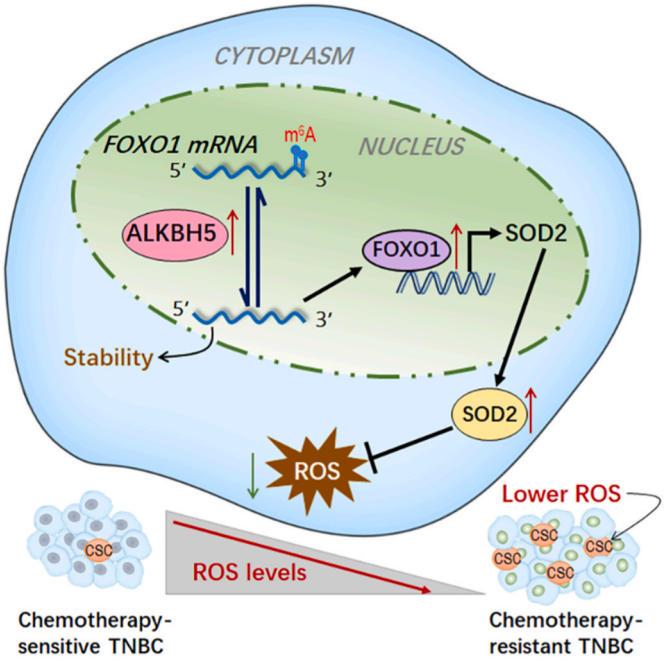

Fig. 7. Proposed model of the mechanism underlying the ALKBH5/FOXO1/SOD2 in maintaining low ROS levels and chemoresistance of TNBC.

Ethics approval and consent to participate

All human-associated tissues used in this research were approved by the Ethics Committee of Affiliated Cancer Hospital and Institute of Guangzhou Medical University. The informed consent has been signed by all patients before their tissues were acquired.

Availability of data and materials

All data generated or analyzed during this study are included in this published article.

Author contributions

Xi. L., P. L., H. Li., and X. Lin. performed the experiments. D. C., Xin. L., and Y. D. interpreted the data and revised the manuscript. Y. H. performed the patients' studies. Xi. L, Y. Z., and H. Liu. designed the experiments and wrote the manuscript. All authors read and approved the final manuscript.

Declaration of Competing Interest

The authors declare no competing interests.

Data availability

Data will be made available on request.

Appendix A. Supplementary data

Supplementary data to this article can be found online at https://doi.org/10.1016/j.redox.2023.102993.

References

[1] S.S. Onkar, N.M. Carleton, P.C. Lucas, T.C. Bruno, A.V. Lee, D.A.A. Vignali, et al., The great immune escape: understanding the divergent immune response in breast cancer subtypes, Cancer Discov. 13 (2023) 23–40.
[2] E. Nolan, G.J. Lindeman, J.E. Visvader, Deciphering breast cancer: from biology to the clinic, Cell 186 (2023) 1708–1728.
[3] L. Yin, J.J. Duan, X.W. Bian, S.C. Yu, Triple-negative breast cancer molecular subtyping and treatment progress, Breast Cancer Res. 22 (2020) 61.
[4] K.A. Won, C. Spruck, Triple-negative breast cancer therapy: current and future perspectives (Review), Int. J. Oncol. 57 (2020) 1245–1261.
[5] O. Metzger, I. Bozovic-Spasojevic, F. Cardoso, Treatment of metastatic breast cancer: an overview, EJHP Pract. 17 (2011) 20–23.
[6] R.H. Wijdeven, B.X. Pang, S.Y. van der Zanden, X.H. Qiao, V. Blomen, M. Hoogstraat, et al., Genome-wide identification and characterization of novel factors conferring resistance to topoisomerase II poisons in cancer, Cancer Res. 75 (2015) 4176–4187.
[7] B.M. Sahoo, B.K. Banik, P. Borah, A. Jain, Reactive oxygen species (ROS): key components in cancer therapies, Anti-Cancer Agent Me 22 (2022) 215–222.
[8] S. Prasad, S.C. Gupta, A.K. Tyagi, Reactive oxygen species (ROS) and cancer: role of antioxidative nutraceuticals, Cancer Lett. 387 (2017) 95–105.
[9] J.N. Moloney, T.G. Cotter, ROS signalling in the biology of cancer, Semin. Cell Dev. Biol. 80 (2018) 50–64.
[10] E.C. Cheung, K.H. Vousden, The role of ROS in tumour development and progression, Nat. Rev. Cancer 22 (2022) 280–297.
[11] Y.C. Chen, Y.L. Li, L.Y. Huang, Y. Du, F.H. Gan, Y.X. Li, et al., Antioxidative stress: inhibiting reactive oxygen species production as a cause of radioresistance and chemoresistance, Oxid. Med. Cell. Longev. 2021 (2021), 6620306.
[12] Q. Cui, J.Q. Wang, Y.G. Assaraf, L. Ren, P. Gupta, L.Y. Wei, et al., Modulating ROS to overcome multidrug resistance in cancer, Drug Resist. Updates 41 (2018) 1–25.
[13] X.L. Jiang, B.Y. Liu, Z. Nie, L.C. Duan, Q.X. Xiong, Z.X. Jin, et al., The role of m6A modification in the biological functions and diseases, Signal Transduct Tar 6 (2021) 74.
[14] X. Wang, Z.K. Lu, A. Gomez, G.C. Hon, Y.N. Yue, D.L. Han, et al., N6-methyladenosine-dependent regulation of messenger RNA stability, Nature 505 (2014) 117–120.
[15] T.Y. Wang, S. Kong, M. Tao, S.Q. Ju, The potential role of RNA N6-methyladenosine in Cancer progression, Mol. Cancer 19 (2020) 88.
[16] X.L. Deng, R. Su, H.Y. Weng, H.L. Huang, Z.J. Li, J.J. Chen, RNA N6-methyladenosine modification in cancers: current status and perspectives, Cell Res. 28 (2018) 507–517.
[17] Z.J. Xu, B. Peng, Y. Cai, G.T. Wu, J.Z. Huang, M. Gao, et al., N6-methyladenosine RNA modification in cancer therapeutic resistance: current status and perspectives, Biochem. Pharmacol. 182 (2020) 148.
[18] Q. Lan, P.Y. Liu, J.L. Bell, J.Y. Wang, S. Hüttelmaier, X.D. Zhang, et al., The emerging roles of RNA m6A methylation and demethylation as critical regulators of tumorigenesis, drug sensitivity, and resistance, Cancer Res. 81 (2021) 3431–3440.
[19] D. Nassar, C. Blanpain, Cancer stem cells: basic concepts and therapeutic implications, Annu Rev Pathol-Mech. 11 (2016) 47–76.
[20] Y.Y. Yan, M. He, L. Zhao, H.Z. Wu, Y.Y. Zhao, L. Han, et al., A novel HIF-2α targeted inhibitor suppresses hypoxia-induced breast cancer stemness via SOD2-mtROS-PDI/GPR78-UPR axis, Cell Death Differ. 29 (2022) 1769–1789.
[21] J.Z. Liu, Y.L. Hu, Y. Feng, Y. Jiang, Y.B. Guo, Y.F. Liu, et al., BDH2 triggers ROS-induced cell death and autophagy by promoting Nrf2 ubiquitination in gastric cancer, J. Exp. Clin. Cancer Res. 39 (2020) 123.
[22] M.P. Jin, J.J. Wang, X.Y. Ji, H.Y. Cao, J.J. Zhu, Y.B. Chen, et al., MCUR1 facilitates epithelial-mesenchymal transition and metastasis via the mitochondrial calcium dependent ROS/Nrf2/Notch pathway in hepatocellular carcinoma, J. Exp. Clin. Cancer Res. 38 (2019) 136.
[23] W.N. Mi, C.Y. Wang, G. Luo, J.H. Li, Y.Z. Zhang, M.M. Jiang, et al., Targeting ERK induced cell death and p53/ROS-dependent protective autophagy in colorectal cancer, Cell Death Dis. 7 (2021) 375.
[24] M. Moeinifard, Z.M. Hassan, F. Fallahian, M. Hamzeloo-Moghadam, M. Taghikhani, Britannin induces apoptosis through AKT-FOXO1 pathway in human pancreatic cancer cells, Biomed. Pharmacother. 94 (2017) 1101–1110.
[25] C.Y. Han, K.B. Cho, H.S. Choi, H.K. Han, K.W. Kang, Role of FoxO1 activation in MDR1 expression in adriamycin-resistant breast cancer cells, Carcinogenesis 29 (2008) 1837–1844.
[26] V. Halytskiy, Multiple drug resistance in breast cancer cells: mirnaome dysregulation can facilitate expression of genes encoding the atp binding cassette (abc) transporters, Breast 36 (2017). S57-S57.
[27] T. Nagashima, N. Shigematsu, R. Maruki, Y. Urano, H. Tanaka, A. Shimaya, et al., Discovery of novel forkhead box O1 inhibitors for treating type 2 diabetes: improvement of fasting glycemia in diabetic/mice, Mol. Pharmacol. 78 (2010) 961–970.
[28] T.C. Chou, Drug combination studies and their synergy quantification using the chou-talalay method, Cancer Res. 70 (2010) 440–446.
[29] C. Kim, R.L. Gao, E. Sei, R. Brandt, J. Hartman, T. Hatschek, et al., Chemoresistance evolution in triple-negative breast cancer delineated by single-cell sequencing, Cell 173 (2018) 879–893.
[30] B.C. Baguley, Multiple drug resistance mechanisms in cancer, Mol. Biotechnol. 46 (2010) 308–316.
[31] T. Ozben, Mechanisms and strategies to overcome multiple drug resistance in cancer, FEBS Lett. 580 (2006) 2903–2909.
[32] L.E. He, H.Y. Li, A.Q. Wu, Y.L. Peng, G. Shu, G. Yin, Functions of N6-methyladenosine and its role in cancer, Mol. Cancer 18 (2019) 176.
[33] Y.W. Wang, H. Qi, Y. Liu, C. Duan, X.L. Liu, T. Xia, et al., The double-edged roles of ROS in cancer prevention and therapy, Theranostics 11 (2021) 4839–4857.
[34] K.S. Chun, D.H. Kim, Y.J. Surh, Role of reductive versus oxidative stress in tumor progression and anticancer drug resistance, Cells 10 (2021) 758.

[35] P. Bragado, A. Armesilla, A. Silva, A. Porras, Apoptosis by cisplatin requires p53 mediated p38α MAPK activation through ROS generation, Apoptosis 12 (2007) 1733–1742.
[36] N. Pilco-Ferreto, G.M. Calaf, Influence of doxorubicin on apoptosis and oxidative stress in breast cancer cell lines, Int. J. Oncol. 49 (2016) 753–762.
[37] A. Parekh, S. Das, S. Parida, C.K. Das, D. Dutta, S.K. Mallick, et al., Multi-nucleated cells use ROS to induce breast cancer chemoresistance in vitro and in vivo, Oncogene 37 (2018) 4546–4561.
[38] X. Qian, X.B. Nie, W.H. Yao, K. Klinghammer, H. Sudhoff, A.M. Kaufmann, et al., Reactive oxygen species in cancer stem cells of head and neck squamous cancer, Semin. Cancer Biol. 53 (2018) 248–257.
[39] K.M. Lee, J.M. Giltnane, J.M. Balko, L.J. Schwarz, A.L. Guerrero-Zotano, K. E. Hutchinson, et al., MYC and MCL1 cooperatively promote chemotherapy-resistant breast cancer stem cells via regulation of mitochondrial oxidative phosphorylation, Cell Metabol. 26 (2017) 633–647.
[40] D. Wang, Y.Q. Wang, X.T. Zou, Y.D. Shi, Q. Liu, T.R. Huyan, et al., FOXO1 inhibition prevents renal ischemia-reperfusion injury via cAMP-response element binding protein/PPAR-γ coactivator-1α-mediated mitochondrial biogenesis, Br. J. Pharmacol. 177 (2020) 432–448.
[41] L.O. Klotz, C. Sánchez-Ramos, I. Prieto-Arroyo, P. Urbánek, H. Steinbrenner, M. Monsalve, Redox regulation of FoxO transcription factors, Redox Biol. 6 (2015) 51–72.
[42] G. Calissi, E.W.F. Lam, W. Link, Therapeutic strategies targeting FOXO transcription factors, Nat. Rev. Drug Discov. 20 (2021) 21–38.
[43] C.W. Pan, X. Jin, Y. Zhao, Y.Q. Pan, J. Yang, R.J. Karnes, et al., AKT-phosphorylated FOXO1 suppresses ERK activation and chemoresistance by disrupting IQGAP1-MAPK interaction, EMBO J. 36 (2017) 995–1010.
[44] J. Park, Y.S. Ko, J. Yoon, M.A. Kim, J.W. Park, W.H. Kim, et al., The forkhead transcription factor FOXO1 mediates cisplatin resistance in gastric cancer cells by activating phosphoinositide 3-kinase/Akt pathway, Gastric Cancer 17 (2014) 423–430.
[45] H.F. Zhang, C.H. Xie, J. Yue, Z.Z. Jiang, R.J. Zhou, R.F. Xie, et al., Cancer-associated fibroblasts mediated chemoresistance by a FOXO1/TGF1 signaling loop in esophageal squamous cell carcinoma, Mol. Carcinog. 56 (2017) 1150–1163.
[46] H. Liu, H. Lyu, G.M. Jiang, D.Y. Chen, S.B. Ruan, S. Liu, et al., ALKBH5-Mediated m6A demethylation of GLUT4 mRNA promotes glycolysis and resistance to HER2-targeted therapy in breast cancer, Cancer Res. 82 (2022) 3974–3986.
[47] C.Z. Zhang, D. Samanta, H.Q. Lu, J.W. Bullen, H.M. Zhang, I. Chen, et al., Hypoxia induces the breast cancer stem cell phenotype by HIF-dependent and ALKBH5-mediated m6A-demethylation of NANOG mRNA, P Natl Acad Sci USA 113 (2016) E2047–E2056.
[48] D.D. Jian, Y. Wang, L.G. Jian, H. Tang, L.X. Rao, K. Chen, et al., METTL14 aggravates endothelial inflammation and atherosclerosis by increasing FOXO1 N6-methyladeosine modifications, Theranostics 10 (2020) 8939–8956.
[49] Z.G. Wang, Y.B. Qi, Y.H. Feng, H.E. Xu, J.X. Wang, L.Y. Zhang, et al., The N6-methyladenosine writer WTAP contributes to the induction of immune tolerance post kidney transplantation by targeting regulatory T cells, Lab. Invest. 102 (2022) 1268–1279.
[50] Y. Yang, F. Shen, W. Huang, S.S. Qin, J.T. Huang, C. Sergi, et al., Glucose is involved in the dynamic regulation of m6A in patients with type 2 diabetes, J. Clin. Endocrinol. Metab. 104 (2019) 665–673.
[51] M.R. Kuracha, V. Govindarajan, B.W. Loggie, M. Tobi, B.L. McVicker, Pictilisib-induced resistance is mediated through FOXO1-dependent activation of receptor tyrosine kinases in mucinous colorectal adenocarcinoma cells, Int. J. Mol. Sci. 24 (2023), 12331.
[52] J.M. Yu, W. Sun, Z.H. Wang, X. Liang, F. Hua, K. Li, et al., TRIB3 supports breast cancer sternness by suppressing FOXO1 degradation and enhancing SOX2 transcription, Nat. Commun. 10 (2019) 5720.